Toward Understanding Tryptophan Fluorescence in Proteins†

Yu Chen and Mary D. Barkley*

Department of Chemistry, Case Western Reserve University, Cleveland, Ohio 44106-7078

Received February 3, 1998; Revised Manuscript Received May 6, 1998

ABSTRACT: A general approach to dissecting the complex photophysics of tryptophan is presented and used to elucidate the effects of amino acid functional groups on tryptophan fluorescence. We have definitively identified the amino acid side chains that quench tryptophan fluorescence and delineated the respective quenching mechanisms in a simple model system. Steady-state and time-resolved fluorescence techniques, photochemical H−D exchange experiments, and transient absorption techniques were used to measure individual contributions to the total nonradiative rate for deactivation of the excited state, including intersystem crossing, solvent quenching, and excited-state proton and electron transfer rates. Eight amino acid side chains representing six functional groups quench 3-methylindole fluorescence with a 100-fold range in quenching rate constant. Lysine and tyrosine side chains quench by excited-state proton transfer; glutamine, asparagine, glutamic and aspartic acid, cysteine, and histidine side chains quench by excited-state electron transfer. These studies provide a framework for deriving detailed structural and dynamical information from tryptophan fluorescence intensity and lifetime data in peptides and proteins.

Fluorescence spectroscopy is widely used to study peptides and proteins. The aromatic amino acids, tryptophan, tyrosine, and phenylalanine, offer intrinsic fluorescent probes of protein conformation, dynamics, and intermolecular interactions. Of the three, tryptophan is the most popular probe. Tryptophan occurs in one or a few residues in most proteins and biologically active peptides. The fluorescence of the indole chromophore is highly sensitive to environment, making it an ideal choice for reporting protein conformation changes and interactions with other molecules. The emission spectrum of tryptophan in proteins varies from a structured band to a broad, diffuse band with wavelength maximum spanning a 40-nm range (*1*). The fluorescence quantum yield ranges from near zero to 0.35. In principle, if the protein structure is known, then changes in tryptophan fluorescence could be interpreted in structural terms at atomic resolution. Unfortunately, the complex photophysics of the indole chromophore have stymied detailed interpretation of protein fluorescence for three decades. However, recent work with constrained tryptophan derivatives (*2*−*7*) and indole model systems (*8*−*11*) promises to make tryptophan fluorescence a more useful structural probe. The environmental sensitivity of the wavelength of the emission maximum is now well understood (*11*). Prospects are excellent for using tryptophan emission spectra to model changes in the local electric field around the indole ring.

The environmental sensitivity of the fluorescence intensity and quantum yield is due to nonradiative processes that compete with emission for deactivation of the excited state. The decay kinetics of the excited singlet state are key to using fluorescence intensity as a structural tool. The fluorescence quantum yield Φ_F and lifetime τ are defined as

$$\Phi_F = k_r/(k_r + k_{nr}) = k_r\tau \quad (1a)$$

$$\tau^{-1} = k_r + k_{nr} \quad (1b)$$

where k_r and k_{nr} are the radiative and nonradiative rates. For tryptophan, k_{nr} may include contributions from several nonradiative processes

$$k_{nr} = k_{isc} + k_{si} + k_{pt} + k_{et} \quad (2)$$

including intersystem crossing k_{isc} (*10*, *12*, *13*), solvent quenching k_{si} (*4*, *14*, *15*), excited-state proton transfer k_{pt} (*8*, *16*−*18*), and excited-state electron transfer k_{et} (*19*, *20*) rates. In proteins, the relative rates of these nonradiative processes depend on the nature and disposition of protein functional groups and water molecules around the tryptophan.

Intersystem crossing as well as photoionization are two nonradiative processes monitored directly by flash photolysis experiments. The intersystem crossing rate of indole is temperature-independent (*13*) but enhanced by heavy atoms. Triplet yields Φ_T are measured with KI, and intersystem crossing rates of $(2-8) \times 10^7$ s^{-1} are calculated from (*10*)

$$k_{isc} = \Phi_T/\tau \quad (3)$$

The k_{isc} values are not affected by the peptide bond. Photoionization to radical and solvated electron is temperature-dependent (*13*). However, it occurs from a prefluorescent state (*21*), so it will affect the fluorescence quantum yield but not the lifetime.

Solvent quenching is an isotopically sensitive temperature-dependent nonradiative process that occurs in all indoles. The temperature dependence of the fluorescence lifetime is expressed by Arrhenius factors

$$\tau^{-1} = k_0 + A \exp(-E^*/RT) \quad (4)$$

† This work was supported by NIH Grant GM42101.

* Address correspondence to this author. E-mail: mdb4@po.cwru.edu.

S0006-2960(98)00274-8 CCC: $15.00
Published on Web 06/24/1998

where k_0 is the temperature-independent rate, A is the frequency factor, and E^* is the activation energy. The temperature-independent rate comprises the radiative rate, intersystem crossing rate, and other temperature-independent nonradiative rates k_{nr}^0

$$k_0 = k_r + k_{isc} + k_{nr}^0 \quad (5)$$

The solvent quenching rate k_{si} is calculated from the Arrhenius parameters

$$k_{si} = A \exp(-E^*/RT) \quad (6)$$

The water quenching rate has about a 2.5-fold deuterium isotope effect and strong temperature dependence with frequency factors of $10^{15}-10^{17}$ s^{-1} and activation energies of 11−13 kcal/mol (*4*, *5*). The large frequency factor suggests electronic motion, though the detailed mechanism is not known. Organic solvent and other solutes as well as a proximal ammonium group decrease the water quenching rate (*5*, *10*, *14*).

Excited-state proton transfer is the best characterized nonradiative process. Three excited-state proton transfer reactions occur, depending on the availability of strong proton donors or acceptors. Below pH 4 the fluorescence is quenched by acid-catalyzed protonation of the indole ring with pK_a* about 2−3 (*22*). Above pH 11 the fluorescence is quenched by base-catalyzed deprotonation of indole NH with pK_a* about 12−13 (*22*). At intermediate pH the fluorescence is quenched by proton exchange at indole C2, C4, and C7 (*8*, *9*, *16*, *17*). (Exchange also occurs at C3 in indole compounds with a hydrogen at this position.) Proton exchange at aromatic carbons on the excited indole ring is catalyzed by good proton donors, such as the ammonium group or trifluoroethanol. The proton transfer yield Φ_{PT} is measured directly by photochemical H−D isotope exchange experiments and k_{pt} is calculated from (*9*, *17*, *18*)

$$k_{pt} = \Phi_{PT}/\tau \quad (7)$$

The proton transfer rate has about a 2−4-fold solvent deuterium isotope effect and modest temperature dependence with frequency factors of 10^{10} s^{-1} and activation energies of about 4 kcal/mol (*8*, *17*).

Excited-state electron transfer from the indole ring to an electrophilic acceptor is the most elusive nonradiative process but probably the most common quenching mechanism in proteins. The evidence for electron transfer is entirely circumstantial, based on correlations between bimolecular quenching rate constant and reduction potential of solute quenchers (*23*, *24*), substitutent effects (*3*, *5*−*7*, *18*, *20*), and intramolecular quenching in peptides and adducts (*25*−*29*). The peptide bond appears to quench tryptophan fluorescence by electron transfer (*10*). The electron transfer rate k_{et} is independent of solvent isotope and weakly temperature dependent with Arrhenius parameters that vary with electron acceptor (*10*).

This paper identifies the protein functional groups that quench tryptophan fluorescence and delineates their respective quenching mechanisms. Quenching rate constants of free amino acids have been reported (*19*, *30*). However, earlier studies failed to account for quenching by the α-amino group. Previously we obtained definitive evidence for peptide bond quenching (*10*). Using a similar strategy here, we determine the effects of amino acid side chains on the individual rates in eq 2 by the methods outlined above. In addition, the relative propensity of amino acid functional groups to accept an electron is gauged from transient absorption experiments monitoring solvated electron. Excited-state electron transfer is inferred from correlations of fluorescence quenching and electron capture rate constants.

MATERIALS AND METHODS

Tryptophan (Sigma) was recrystallized four times from 70% ethanol. *N*-Acetyltyrosine (Sigma) was recrystallized from water. Other chemicals (highest grade) from Sigma or Aldrich were used as received. pK_as of *N*-acetyl amino acids were determined by titration with a pH meter.

Fluorescence. Steady-state and time-resolved fluorescence measurements are described elsewhere (*4*, *10*). Fluorescence was measured at 288-nm excitation wavelength on solutions of absorbance < 0.1. Absorbance was measured on a Cary 3E UV−vis spectrophotometer. Fluorescence quantum yields Φ_F were measured relative to that of tryptophan in water with a value of 0.14 at 25 °C (*31*). Fluorescence quenching rate constants k_q are calculated from relative quantum yield or lifetime data in the absence and presence of quencher Q by using the Stern−Volmer equation

$$\Phi_{F0}/\Phi_F = \tau_0/\tau = 1 + k_q\tau_0[Q] \quad (8)$$

where the subscript 0 denotes absence of quencher. Longer excitation wavelengths were used to reduce absorption by the following quenchers: *N*-acetylcysteine (304 nm), *N*-acetyltyrosine and phenol in H_2O (305 nm), and *N*-acetyltyrosine in D_2O (312 nm). Fluorescence decays were measured at 370- or 390-nm emission wavelength (8-nm band-pass) and deconvolved as described elsewhere (*10*). *N*-Acetylcysteine solutions were prepared and used within 1 day. After 2 days, the pH of solutions containing *N*-acetylcysteine decreased and the k_q value increased, presumably due to formation of *N*-acetylcystine.

Transient Absorbance. Laser flash photolysis measurements are described elsewhere (*10*). Transient absorbance was measured on deoxygenated solutions of $A_{280} = 0.6-0.8$ [$(1-2) \times 10^{-4}$ M 3-methylindole] in 1 cm cells at ∼25 °C. Triplet quantum yields Φ_T were measured relative to that of 3-methylindole in water with a value of 0.18 (*10*). Intersystem crossing rates k_{isc} are calculated from eq 3 by using fluorescence lifetimes τ for deoxygenated solutions. The solvated electron was generated from photoionization of 3-methylindole and monitored at 680 nm. The transient absorbance was fit to a single-exponential decay. Bimolecular rate constants k_e for capture of solvated electron are calculated from the lifetime of solvated electron in the absence τ_{e0} and presence τ_e of fluorescent quencher Q according to

$$\tau_{e0}/\tau_e = 1 + k_e\tau_{e0}[Q] \quad (9)$$

The quencher concentration was <0.1 M.

H−D Exchange. Photochemical isotope exchange measurements are described elsewhere (*8*, *9*). Samples were irradiated with a Spectral Energy LH150 xenon lamp. H−D exchange was monitored by mass spectrometry on a Hewlett-

Table 1: Quenching of 3-Methylindole Fluorescence

quencher	solvent	$k_q \times 10^7$ M^{-1} s^{-1} Φ_{F_0}/Φ_F[a]	$k_q \times 10^7$ M^{-1} s^{-1} τ_0/τ	$k_{isc} \times 10^7$ s^{-1}	$k_{si} \times 10^7$ s^{-1} [b] at 25 °C
N-acetyl-Lys	H_2O, pH 5.4	10	10		4.3 (4.7)
pK_a 10.5	D_2O, pD 5.6	3.4			
glycine	H_2O, pH 6.5	26[c]		2.0	
	D_2O, pD 6.5	6.0[c]			
N-acetyl-Tyr[d]	H_2O, pH 5.3	98 ± 6			
	D_2O, pD 5.3	48			
phenol	H_2O, pH 5.4	89	89		
pK_a 9.89	D_2O, pD 5.6	42	42		
N-acetyl-Gln	H_2O, pH 7.0	2.2 ± 0.2[e]			
	D_2O, pD 7.4	2.0			
NAGA	H_2O, pH 5.1	6.6 ± 0.3[e]	6.4	2.0[e]	3.8 (3.8)[e]
	D_2O, pD 5.3	6.5[e]			1.6 (1.8)[e]
N-acetyl-Asn	H_2O, pH 7.0	8.8 ± 0.3[e]			
CH_3COOH[f]	H_2O, pH 4.7	43 ± 2	43	1.8 ± 0.4	
pK_a 4.7	D_2O, pD 4.7	42			
N-acetyl-Cys	H_2O, pH 7.6	140 ± 10	140		4.9
pK_a 3.2, 9.3	D_2O, pD 7.6	97			
	H_2O, pH 10.4	190 ± 10	180		
	D_2O, pD 10.4	140			
Cys−Cys	H_2O, pH 10.0	>1000			
N-acetyl-His	H_2O, pH 5.3	240 ± 20	230		5.4
pK_a 3.4, 7.2	D_2O, pD 5.6	210			
	H_2O, pH 9.7	3.7 ± 0.5			
	D_2O, pD 9.7	3.1			
acrylamide	H_2O, pH 7.0	720			

[a] Lifetime of 3-methylindole is 8.2 ns in H_2O and 12.0 ns in D_2O at 25 °C, oxygenated solution. [b] In the absence of quencher, $k_{si} = 5.9 \times 10^7$ s^{-1} at 25 °C. Number in parentheses is k_{si} in the presence of an equal concentration of control compound that does not quench 3-methylindole fluorescence. [c] Data from ref *8*. [d] Recrystallized *N*-acetyl-Tyr contained a fluorescent impurity with emission maximum at 400 nm, probably a dityrosine derivative. Background fluorescence was subtracted. Background fluorescence was 3% in 3-methylindole solutions containing 0.05 M *N*-acetyl-Tyr. Phenol was used to confirm the k_q values of the tyrosine side chain. [e] Data from ref *10*. [f] Values were corrected for partial dissociation.

Packard 5970 GC-MS. The fraction of H−D exchange ϕ_{ex} was determined from the increase in the peak at *m*/*z* 133

$$\phi_{ex} = (I_{133} - k_{nr}^0 I_{133}^0)/(I_{132}^0 - I_{133}^0) \qquad (10)$$

where I_{132}^0 and I_{133}^0 are the total intensities at *m*/*z* 132 and 133 in freshly prepared unirradiated samples and I_{133} is the total intensity at *m*/*z* 133 in an irradiated sample. Irradiation conditions were chosen so that a second H−D exchange per molecule was negligible. The proton transfer yield Φ_{PT} was determined by photoactinometry and the proton transfer rate k_{pt} was calculated from eq 7.

RESULTS

Previously we showed that the ammonium but not carboxylate of free amino acids quenches the fluorescence of 3-methylindole (*8*). We also showed that a single amide group as in *N*-acetylglycine quenches too weakly to be detected in a bimolecular quenching experiment (*10*). Therefore, simple Stern−Volmer quenching experiments with *N*-acetyl amino acids and 3-methylindole should unambiguously identify which amino acid side chains quench tryptophan fluorescence (Table 1). Additional experiments delineate the quenching mechanisms. Besides nonradiative processes, ground-state interactions could cause quenching. This would increase the fluorescence quenching rate constant k_q determined from quantum yield data compared to the k_q value from lifetime data. Ground-state complexes between the indole ring and amino acid side chains affect the absorption spectrum of indole (*26*).

Quenching due to enhancement of intersystem crossing was checked in transient absorption experiments. The triplet quantum yield Φ_T and fluorescence lifetime τ were measured on deoxygenated solutions of 3-methylindole in the presence of *N*-acetyl amino acids and used to calculate the intersystem crossing rate k_{isc}. In many cases, the *N*-acetyl amino acid quenched the triplet too, making it difficult or impossible to measure initial absorbance accurately. In the few instances where we were able to measure Φ_T, we saw no changes in k_{isc} value. Quenching due to acceleration of solvent quenching was checked by measuring the temperature dependence of the fluorescence lifetime in the presence of *N*-acetyl amino acids. A second Arrhenius factor was included in eq 4 to account for a second temperature-dependent nonradiative process, such as proton or electron transfer.

Excited-state proton transfer was diagnosed by measuring quenching rate constants in both H_2O and D_2O. A large deuterium isotope effect on k_q indicates a proton transfer reaction. Photochemical isotope exchange experiments confirmed proton transfer and measured the rate constant k_{pt}. Excited-state electron transfer was inferred by default for quenching rate constants k_q that were not accounted for by the other mechanisms. In addition, the rate of electron capture by *N*-acetyl amino acids was measured. Figure 1 shows the transient absorbance of solvated electron in the absence and presence of an *N*-acetyl amino acid that quenches 3-methylindole fluorescence. The bimolecular rate constant for quenching of solvated electron k_e was calculated from eq 9 (Table 2).

Nonquenching Side Chains. Quenching of 3-methylindole fluorescence by *N*-acetyl derivatives of glycine, alanine, valine, leucine, phenylalanine, proline, hydroxyproline, serine, threonine, methionine, and arginine at neutral pH is not detectable. The lower limit for detection in intermo-

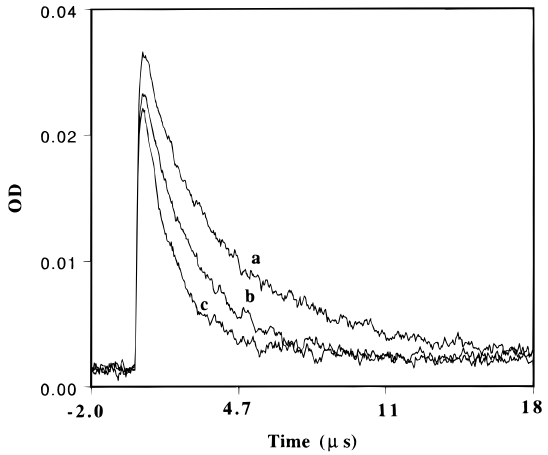

FIGURE 1: Transient absorption spectra of solvated electron in (a) H_2O; (b) 2.7 mM *N*-acetylhistidine, pH 9.4; and (c) 0.17 mM *N*-acetylhistidine, pH 5.3.

Table 2: Bimolecular Rate Constants

quencher	pH	$k_e \times 10^7$ M^{-1} s^{-1} [a]	$k_{et} \times 10^7$ M^{-1} s^{-1} at 25 °C
N-acetyl-Met	7.0	0.22	
Gly	7.0	0.65	0
N-acetyl-Lys	5.4	0.69	0
N-acetyl-Gln	7.0	3.9	2.2
NAGA	7.0	8.3	6.6
N-acetyl-Asn	7.0	24	8.8[b]
CH_3COOH[c]	4.7	61	43
N-acetyl-Cys	7.6	440	10.5
	10.5	220	
N-acetyl-His	5.3	220	
	9.4	5.0	

[a] 25 °C, deoxygenated solution. [b] Data from ref *10*. [c] Values were corrected for partial dissociation.

lecular quenching experiments is $k_q \sim 1 \times 10^7$ M^{-1} s^{-1}. All of the parent amino acids except leucine and phenylalanine were previously reported to quench tryptophan fluorescence at pH 5−6, purportedly by excited-state electron transfer (*19*, *32*, *33*). We subsequently showed that glycine quenches indole fluorescence by excited-state proton transfer (*8*). By analogy with glycine, the quenching observed for the free amino acids is due to excited-state proton transfer catalyzed by the protonated α-amino group. It is not due to the side chains or carboxylate. Finally, we measured the electron capture rate for one nonquenching *N*-acetyl derivative and obtained a very low value (Table 2).

Proton Transfer Quenching Side Chains. Quenching of 3-methylindole fluorescence by *N*-acetyllysine and *N*-acetyltyrosine is isotopically sensitive. The 2−3-fold deuterium isotope effect on k_q indicates quenching by excited-state proton transfer. Quenching by the α-amino group of glycine was also isotopically sensitive with a 4-fold deuterium isotope effect on k_q (*8*). Excited-state proton transfer was confirmed for *N*-acetyllysine by photochemical H−D exchange. The photochemical yield for isotope exchange of 3-methylindole in D_2O, pD 7, with 0.5 M *N*-acetyllysine was $\phi_{ex} = 0.13$. The bimolecular rate constant for proton transfer is estimated to be $k_{pt} = (3.8 \pm 0.8) \times 10^7$ M^{-1} s^{-1}, which is close to the Stern−Volmer rate constant k_q for fluorescence quenching (Table 1). The strong UV absorption of *N*-acetyltyrosine and phenol precludes H−D exchange experiments in the presence of these quenchers.

Transient absorption experiments in the presence of *N*-acetyllysine show that the intersystem crossing rate is unchanged (Table 1) and that the lysine side chain is a poor electron acceptor (Table 2). The strong UV absorption of *N*-acetyltyrosine and phenol also precludes transient absorption experiments in the presence of these quenchers.

Electron Transfer Quenching. Both *N*-acetylglutamine and *N*-acetylasparagine quench 3-methylindole fluorescence weakly with a negligible deuterium isotope effect. The quenching properties of the amide group were characterized previously (*10*). Two amide groups are needed for detectable intermolecular quenching. The quenching rate constant k_q increases with decreasing distance between the two groups. The quenching mechanism was proposed to be excited-state electron transfer.

Quenching by the side chains of glutamic and aspartic acids was not assessed with *N*-acetyl derivatives. The presence of two carboxyl groups with pK_a values in the region pH 2−4 makes it harder to define the protonation state around pH 4. Instead, acetic acid with pK_a = 4.7 was used as a model for quenching by carboxylic acid side chains. Only the protonated carboxyl quenched 3-methylindole fluorescence and there was no deuterium isotope effect on k_q (Table 1), in agreement with previous findings for indole (*24*).

N-Acetylcysteine is a strong quencher of 3-methylindole fluorescence, though not as strong as acrylamide, which quenches at the diffusion limit (Table 1). The k_q value of *N*-acetylcysteine increased about 35% in the thiolate compared to the thiol with a 1.4-fold deuterium isotope effect for both ionization states. The quenching rate constants were measured over a concentration range of 0.005−0.1 M *N*-acetylcysteine. Slight changes in the absorption spectra of 3-methylindole in the presence of ≥0.1 M *N*-acetylcysteine reveal a weak ground-state interaction between 3-methylindole and the cysteine side chain. The difference spectra showed two small peaks at 283 and 292 nm. The dependence of absorption spectral changes on *N*-acetylcysteine concentration suggests a stronger ground-state interaction for the thiol than the thiolate. Fluorescence decays of 3-methylindole in the presence of thiol gave somewhat better fits to biexponential than to monoexponential functions. The minor second lifetime component has a 0.25−0.4-ps lifetime and <10% amplitude at 0.1 M *N*-acetylcysteine. The biexponential decay with a short lifetime component may be due to the transient term in k_q (*34*) as well as the ground-state complex. Fluorescence decays of 3-methylindole in the presence of thiolate were monoexponential. For both thiol and thiolate, the k_q values calculated from average lifetime and quantum yield data are identical, indicating that the dominant quenching process occurs in the excited state. Cystine appears to be a very strong quencher, but low solubility in water makes it difficult to measure k_q accurately.

N-Acetylhistidine is also a strong quencher of 3-methylindole fluorescence, but only when the imidazole ring is protonated. The k_q value drops about a factor of 65 upon deprotonation with a scant 1.1−1.2-fold deuterium isotope effect in both ionization states. As in the case of *N*-acetylcysteine, quenching rate constants were measured over a concentration range of 0.005−0.1 M *N*-acetylhistidine. Slight changes were observed in the absorption spectra of 3-methylindole in the presence of ≥0.2 M *N*-acetylhistidine

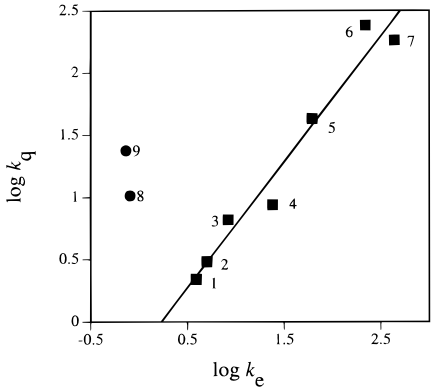

FIGURE 2: Correlation of rate constants for fluorescence quenching k_q and electron capture k_e. (1) *N*-Acetyl-Gln; (2) *N*-acetyl-His, pH 9.4; (3) NAGA; (4) *N*-acetyl-Asn; (5) CH_3COOH; (6) *N*-acetyl-His, pH 5.3; (7) *N*-acetyl-Cys, pH 7.6; (8) *N*-acetyl-Lys; (9) Gly.

with two small peaks in the difference spectra at 283 and 292 nm. The dependence of absorption spectral changes on *N*-acetylhistidine concentration suggests a stronger ground-state interaction for protonated than deprotonated imidazole. The fluorescence decay of 3-methylindole in the presence of *N*-acetylhistidine is biexponential. Like *N*-acetylcysteine, the minor component for protonated imidazole has a 0.25−0.4-ns lifetime and <10% amplitude at 0.1 M *N*-acetylhistidine. The average lifetime drop also parallels the quantum yield drop.

The *N*-acetyl derivatives of glutamine, asparagine, cysteine, and histidine as well as acetic acid quench solvated electron with rate constants that range from about 4×10^7 M^{-1} s^{-1} for *N*-acetylglutamine to 4×10^9 M^{-1} s^{-1} for *N*-acetylcysteine (Table 2). Braams (*35*) measured rate constants for the reaction between solvated electron and free amino acids in pulse radiolysis experiments. His values for cysteine and histidine with protonated side chains are roughly 2-fold higher than ours. The electron capture rate constant for glycine is $<10^7$ M^{-1} s^{-1}. The positively charged α-amino group in the free amino acid may enhance the ability of the sulfhydryl and imidazolium groups to capture the electron compared to the *N*-acetyl derivative.

The likely quenching mechanism for the side chains of glutamine, asparagine, glutamic and aspartic acids, cysteine, cystine, and histidine is excited-state electron transfer. Intuitively, the ability of a compound to capture an electron should be related to its ability to act as an electron acceptor, even though reacting with solvated electron and accepting an electron from excited indole are distinct processes. Thus, the quenching rate constant k_q should be proportional to the electron capture rate constant k_e for compounds that quench 3-methylindole fluorescence by an electron transfer mechanism. Figure 2 plots log k_q vs log k_e and shows good correlation between k_q and k_e in all cases except *N*-acetyllysine and the free amino acid glycine, both of which quench indole fluorescence by excited-state proton transfer. Particular compounds may have more than one quenching mechanism; for example, *N*-acetylcysteine and *N*-acetylhistidine form ground-state complexes. However, contributions from such minor quenching processes do not mask the trend. Large deviations as in the case of *N*-acetyllysine and glycine point to other quenching mechanisms.

Assuming an electron transfer mechanism, the quenching rate constant k_q gives a reasonable estimate of the bimolecular electron transfer rate constant k_{et} when electron transfer is the rate-limiting step in the quenching process. The electron transfer rates are listed in Table 2 for compounds with k_q values well below the diffusion limit of 7×10^9 M^{-1} s^{-1}.

DISCUSSION

Eight side chains of naturally occurring amino acids quench 3-methylindole fluorescence strongly enough to detect in bimolecular quenching experiments: the amide groups of glutamine and asparagine, the carboxyl groups of glutamic and aspartic acids, lysine ϵ-amino group, tyrosine phenol, cysteine sulfhydryl, and histidine imidazole. The quenching reported previously for other amino acids (*19*, *32*, *33*) is due to excited-state proton transfer catalyzed by the α-amino group of the free amino acids. Quenching by the α-amino group of glutamine, asparagine, and lysine also contributes significantly to the quenching rate constants k_q and changes the order of effectiveness of the more weakly quenching side chains.

The eight side chains each have essentially a single quenching mechanism as detected in bimolecular quenching experiments. Ground-state complexes were apparent for only two amino acid side chains: cysteine and histidine. However, the parallel drops in fluorescence quantum yield and lifetime indicate that these weak ground-state interactions have almost no effect on k_q values. The red shift in the absorption spectra of 3-methylindole suggests an indole to side chain charge transfer in the ground-state complex. None of the quenching side chains appears to alter the water quenching rate k_{si} much beyond a small solute effect at high solute concentrations. Also, amino acid functional groups do not enhance the intersystem crossing rate in the few cases where we measured it. The side chains of lysine and probably also tyrosine quench by excited-state proton transfer. The remaining side chains presumably quench by excited-state electron transfer. The small solvent isotope effects on the k_q values for both ionization states of the cysteine and histidine side chains may reflect isotope effects on the electron transfer rate, which approaches the diffusion limit in the case of these side chains. The arguments for electron transfer quenching of tryptophan fluorescence are three. First, we excluded all other known nonradiative processes that quench indole fluorescence, leaving electron transfer as a plausible mechanism. Second, we showed excellent correlation between the relative abilities to quench indole fluorescence and to capture solvated electrons for amino acid functional groups that do not quench by excited-state proton transfer. And third, fluorescence quenching by putative electron acceptors shows the predicted dependence of k_q on redox potential $E°$ of quencher. The electron transfer rate depends exponentially on the driving force for the reaction, which in turn depends on the difference in redox potential between acceptor and donor (*36*). The quenching rate becomes diffusion-limited for strong oxidizing agents, where electron transfer is much faster than diffusion. Figure 3 illustrates this behavior for indole and a variety of quenchers with known values of the redox potential in aqueous solution.

The lifetime of tryptophan in proteins varies from a few hundred picoseconds to 9 ns. Two common quenchers of tryptophan fluorescence are water molecules and peptide

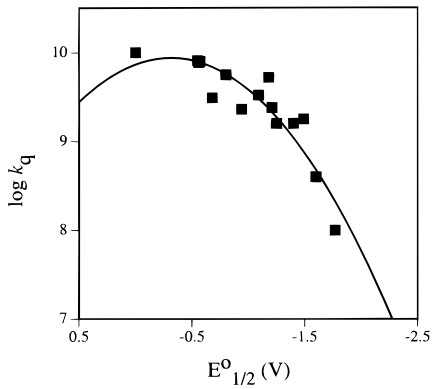

FIGURE 3: Dependence of fluorescence quenching rate constant k_q of indole on redox potential $E°$ of quencher. Quenchers in decreasing order of reduction potential: trichloroacetamide (*37*), dichloroacetamide (*37*), dichloroacetic acid (*24*), trifluoroacetyl ethyl ester, acrylamide (*19*), difluoroacetyl ethyl ester, chloroacetamide (*37*), chloroacetic acid (*24*), 3-chloropropionic acid (*24*), formic acid (*24*), Yb^{3+} (*23*; no heavy atom effect), fluoroacetyl ethyl ester, Gd^{3+} (k_q value corrected for heavy atom effect; *10*). Redox potentials are from refs *23* and *38*. Line drawn is polynomial fit of order 2 predicted by electron transfer theory (*36*).

bonds, which we have discussed previously (*4*, *10*). On the basis of the bimolecular quenching studies in aqueous solution presented here, the side chains of lysine, glutamine, asparagine, and neutral histidine should be relatively weak quenchers; neutral glutamic and aspartic acids should be moderate quenchers; and tyrosine, cysteine, positively charged histidine, and cystine should be the best quenchers in proteins. The proximity of the indole ring to these quenching side chains would affect the fluorescence lifetime. A cautionary word is necessary for glutamic and aspartic acids and histidine. The ionization state of these side chains has a profound effect on quenching ability, and these residues often have anomalous pK_a values in proteins.

In proteins, proximity, specific geometry, or local polarity might enhance the quenching ability of additional amino acid side chains, for example, negatively charged glutamic and aspartic acids, serine, threonine, methionine, and arginine. Proximity and orientation will undoubtedly enhance or suppress particular quenching mechanisms. Ground-state interactions may become more significant in folded proteins, where amino acid functional groups surround the indole ring. Excited-state proton exchange likely has fairly restrictive geometric requirements. Namely, the proton donor must contact the C2, C4, or C7 positions on the indole ring in the correct orientation to catalyze exchange. It is not yet known whether lysine and tyrosine side chains can quench tryptophan fluorescence in peptides and proteins by proton exchange. Excited-state electron transfer, on the other hand, has less stringent structural requirements and is therefore likely to be a major quenching mechanism in peptides and proteins. In principle, electron transfer may occur through-space or through-bond over distances as great as about 10 Å. Finally, although a single mechanism dominates side-chain quenching in bimolecular quenching experiments, tryptophan in proteins will be susceptible to multiple quenching interactions. The tools we have developed to dissect the various contributions to the nonradiative rate should prove applicable in more complex environments. Studies are currently underway to extend this approach to intramolecular quenching in peptides.

REFERENCES

1. Eftink, M. R. (1991) in *Methods of Biochemical Analysis* (Suelter, C. H., Ed.) Vol. 35, pp 127−205, John Wiley and Sons, New York.
2. Tilstra, L., Sattler, M. C., Cherry, W. R., and Barkley, M. D. (1990) *J. Am. Chem. Soc. 112*, 9176−9182.
3. Colucci, W. J., Tilstra, L., Sattler, M. C., Fronczek, F. R., and Barkley, M. D. (1990) *J. Am. Chem. Soc. 112*, 9182−9190.
4. McMahon, L. P., Colucci, W. J., McLaughlin, M. L., and Barkley, M. D. (1992) *J. Am. Chem. Soc. 114*, 8442−8448.
5. Yu, H.-T., Vela, M. A., Fronczek, F. R., McLaughlin, M. L., and Barkley, M. D. (1995) *J. Am. Chem. Soc. 117*, 348−357.
6. Eftink, M. R., Jia, Y., Hu, D., and Ghiron, C. A. (1995) *J. Phys. Chem. 99*, 5713−5723.
7. McMahon, L. P., Yu, H.-T., Shui, L., Fronczek, F. R., McLaughlin, M. L., and Barkley, M. D. (1997) *J. Phys. Chem. 101*, 3269−3280.
8. Yu, H.-T., Colucci, W. J., McLaughlin, M. L., and Barkley, M. D. (1992) *J. Am. Chem. Soc. 114*, 8449−8454.
9. Chen, Y., Liu, B., and Barkley, M. D. (1995) *J. Am. Chem. Soc. 117*, 5608−5609.
10. Chen, Y., Liu, B., Yu, H.-T., and Barkley, M. D. (1996) *J. Am. Chem. Soc. 118*, 9271−9278.
11. Callis, P. R. (1997) *Methods Enzymol. 278*, 113−150.
12. Bent, D. V., and Hayon, E. (1975) *J. Am. Chem. Soc. 97*, 2612−2619.
13. Klein, R., Tatischeff, I., Bazin, M., and Santus, R. (1981) *J. Phys. Chem. 85*, 670−677.
14. Lee, J., and Robinson, G. W. (1984) *J. Chem. Phys. 81*, 1203−1208.
15. Lee, J., and Robinson, G. W. (1985) *J. Phys. Chem. 89*, 1872−1875.
16. Saito, I., Sugiyama, H., Yamamoto, A., Muramatsu, S., and Matsuura, T. (1984) *J. Am. Chem. Soc. 106*, 4286−4287.
17. Shizuka, H., Serizawa, M., Kobayashi, H., Kameta, K., Sugiyama, H., Matsuura, T., and Saito, I. (1988) *J. Am. Chem. Soc. 110*, 1726−1732.
18. Shizuka, H., Serizawa, M., Shimo, T., Saito, I., and Matsuura, T. (1988) *J. Am. Chem. Soc. 110*, 1930−1934.
19. Steiner, R. F., and Kirby, E. P. (1969) *J. Phys. Chem. 73*, 4130−4135.
20. Petrich, J. W., Chang, M. C., McDonald, D. B., and Fleming, G. R. (1983) *J. Am. Chem. Soc. 105*, 3824−3832.
21. Mialocq, J. C., Amouyal, E., Bernas, A., and Grand, D. (1982) *J. Phys. Chem. 86*, 3173−3177.
22. Vander Donckt, E. (1969) *Bull. Soc. Chim. Belges 78*, 69−75.
23. Ricci, R. W., and Kilichowski, K. B. (1974) *J. Phys. Chem. 78*, 1953−1956.
24. Ricci, R. W., and Nesta, J. M. (1976) *J. Phys. Chem. 80*, 974−980.
25. Shinitzky, M., and Goldman, R. (1967) *Eur. J. Biochem. 3*, 139−144.
26. Shinitzky, M., and Fridkin, M. (1969) *Eur. J. Biochem. 9*, 176−181.
27. Eftink, M. R., Jia, Y.-W., Graves, D. E., Wiczk, W., Gryczynski, I., and Lakowicz, H. R. (1989) *Photochem. Photobiol. 49*, 725−729.
28. Bivin, D. B., Kubota, S., Pearlstein, R., and Morales, M. F. (1993) *Proc. Natl. Acad. Sci. U.S.A. 90*, 6791−6795.
29. Bivin, D. B., and Khoroshev, M. I. (1994) *Photochem. Photobiol. A: Chem. 78*, 209−214.
30. Harris, D. L., and Hudson, B. S. (1990) *Biochemistry 29*, 5276−5285.
31. Chen, R. F. (1967) *Anal. Lett. 1*, 35−42.
32. Bohorquez, M. D. V., Cosa, J. J., Garcia, N. A., and Previtali, C. M. (1984) *Photochem. Photobiol. 40*, 201−205.
33. Van Gilst, M., Tang, C., Roth, A., and Hudson, B. (1994) *J. Fluoresc. 4*, 203−207.
34. Lakowicz, J. R., Johnson, M. L., Gryczynski, I., Joshi, N., and Laczko, G. (1987) *J. Phys. Chem. 91*, 3277−3285.

35. Braams, R. (1966) *Radiat. Res. 27*, 319−329.
36. Marcus, R. A., and Sutin, N. (1985) *Biochim. Biophys. Acta 811*, 265−322.
37. Froelich, P. M., and Nelson, K. (1978) *J. Phys. Chem. 82*, 2401−2403.
38. Meites, L., and Zuman, P. (1977−1982) *CRC Handbook Series in Organic Electrochemistry*, Vols. 1−5, CRC Press, Boca Raton, FL.

BI980274N